V.V. KURYLIUK, S.S. SEMCHUK, A.M. KURYLIUK, P.P. KOGUTYUK

Taras Shevchenko National University of Kyiv, Faculty of Physics
(64/13, Volodymyrs'ka Str., Kyiv 01601, Ukraine; e-mail: kuryluk@univ.kiev.ua)

THERMAL CONDUCTIVITY OF SI NANOWIRES WITH AN AMORPHOUS SiO₂ SHELL: A MOLECULAR DYNAMICS STUDY

The processes of thermal transport in Si nanowires covered with an amorphous SiO₂ shell have been studied using the nonequilibrium molecular dynamics method. The influence of the amorphous layer thickness, radius of the crystalline silicon core, and temperature on the thermal conductivity of the nanowires is considered. It is found that the increase of the amorphous shell thickness diminishes the thermal conductivity in Si/SiO₂ nanowires of the core-shell type. The results obtained also testify that the thermal conductivity of Si/SiO₂ nanowires at 300 K increases with the cross-section area of the crystalline Si core. The temperature dependence of the thermal conductivity coefficient in Si/SiO₂ nanowires of the core-shell type is found to be considerably weaker than that in crystalline silicon nanowires. This difference was shown to result from different dominant mechanisms of phonon scattering in those nanowires. The results obtained demonstrate that Si/SiO₂ nanowires are a promising material for thermoelectric applications.

K e y w o r d s: thermal conductivity, nanowire, silicon, molecular dynamics.

1. Introduction

During the last decade, silicon nanowires have been permanently integrated into modern electronic, sensor, and optoelectronic techniques. The unique physical properties of nanowires, on the one hand, and the compatibility of the methods of their synthesis with the available silicon technology, on the other hand, favor the intensive development of nanowire researches and their implementation in various fields. In particular, Si nanowires are considered as a basis for the manufacture of field-effect transistors [1], solar cells [2], and ultrasensitive electro-mechanical and biological sensors [3]. Prospects for the application of silicon wires to improve the functional parameters of light-emitting devices [4] and lithium-ion batteries [5] are actively studied.

A separate direction of modern researches is the study of the capabilities of Si nanostructures to increase the efficiency of energy conversion in thermoelectric elements [6–8]. It is known that the efficiency of thermoelectric element is determined by a dimensionless quantity, the figure of merit ZT [9]

$$ZT = \frac{S^2 \sigma T}{k},\qquad(1)$$

where S is the Seebeck coefficient, σ the specific electrical conductance, k the thermal conductivity, and T the temperature. As follows from formula (1), one of the ways to elevate the efficiency of thermoelectric conversion consists in reducing the thermal conductivity of the working material without inserting substantial changes into its electrical conductivity. Semiconductor nanowires allow the thermal conductivity to be properly modified owing to their developed surface, which serves as an additional source of phonon
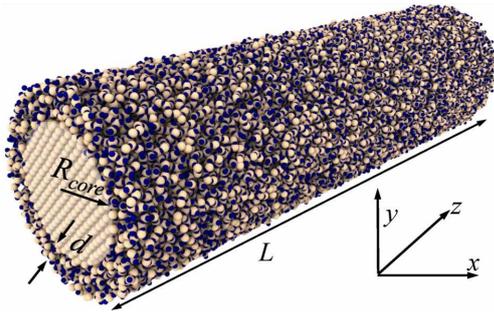
Fig. 1. Geometry of the Si/SiO$_2$ core-shell nanowire. Si and O atoms are exhibited by light and dark circles, respectively

scattering. In particular, it was found experimentally that the ZT value in silicon nanowires with a rough surface approaches unity ($ZT \to 1$) because of an almost 100-fold reduction in their thermal conductivity k as compared with its counterpart in bulk Si [10].

In order to further elevate the figure of merit ZT, the authors of a number of theoretical works proposed a wide range of methods aimed at reducing the thermal conductivity of nanowires. In particular, those methods include the optimization of geometric parameters (such as the cross-section [11], the crystallographic orientation [12], and the degree of structure porosity [13]), the variation of the composite [14] and defect [15] content in nanowires, their deformation [16], and the creation of superlattices [17]. On the other hand, modern experimental studies also open up new ways to control the value of the thermal conductivity k in nanowires. In particular, using the Raman scattering method, a strong anisotropy of k was found in arrays of silicon nanowires [18], which allows the thermal conductivity of the material to be controllably varied by appropriately selecting the heat flow direction. A not less effective way to reduce the thermal conductivity of Si nanowires is the synthesis of structures with a rough surface [19]. In recent experiments with silicon nanowires, a possibility was demonstrated to vary their thermal conductivity within a wide interval of values either by non-uniformly distributing the doping impurities in nanowires [20] or by choosing the doping level for the Si substrates on which the nanowires are synthesized [21].

Another method of reducing the thermal conductivity of nanowires consists in the application of structures with the core-shell architecture, in particular, Si/Ge nanowires [22]. In particular, it was shown that the deposition of a thin Ge shell on a silicon nanowire stimulates a reduction in the nanowire thermal conductivity by about 75% [23]. The transformation of the crystalline shell into the amorphous one by amorphizing the surface Si layer can enhance the reduction of the thermal conductivity to 80% [24]. But the physical mechanisms responsible for a reduction of the thermal conductivity in such nanowires, as well as the prospects of their application in thermoelectric devices, are far from being analyzed at length.

An amorphous shell around a silicon nanowire core can be relatively easily produced in the process of nanowire synthesis through the formation of a layer of natural SiO$_2$ oxide with a varied thickness. In this work, the thermal properties of silicon nanowires with an amorphous SiO$_2$ shell are studied. In particular, using the method of nonequilibrium molecular dynamics, the influence of the SiO$_2$ shell thickness on the thermal conductivity of nanowires and its temperature dependence is considered. The obtained data were analyzed in terms of the phonon scattering processes at the crystalline core/amorphous shell interface.

2. Research Technique

The processes of heat transfer in a cylindrical nanowire consisting of a crystalline silicon core with the radius R_{core} and surrounded by an external amorphous SiO$_2$ shell with the thickness d were studied (Fig. 1). At the first stage of constructing the model structure, a continuous nanowire of amorphous SiO$_2$ was generated. For this purpose, the structure of crystalline α-SiO$_2$ quartz of trigonal syngony with the lattice parameters $a = 4.19$ Å and $c = 5.40$ Å was used. The amorphization was performed by holding the system at the temperature $T = 3000$ K and, afterward, by subjecting it to the drastic cooling (10^{11} K/s) to $T = 300$ K under the conditions of a Langevin thermostat. Afterward, all Si and O atoms located within the radius R_{core} from the axis of the amorphous nanowire were removed, so that a cylindrical cavity was created. This cavity was filled with Si atoms located at the crystal lattice sites.

The heat transfer processes in nanowires were simulated using the molecular dynamics software package LAMMPS [25]. Periodic boundary conditions were imposed at the faces perpendicular to the nanowire axis, whereas the lateral surface was considered free. The examined structure had been held at con-

stant pressure and temperature (the NPT ensemble) for 250 ps until the complete relaxation of mechanical stresses is attained. The equations of motion were integrated with a time increment of 0.5 fs. The interaction between the atoms in the nanowires was described using the Tersoff empirical potential [26]. Its application brings about satisfactory results, when considering heat transfer processes in nanostructures on the basis of amorphous SiO_2 with silicon [27] or germanium [28].

The thermal conductivity coefficient k was determined along the axis of researched cylindrical nanowires (the Oz direction in Fig. 1). Its calculations were carried in the framework of the nonequilibrium molecular dynamics method using the Müller–Plathe algorithm [29]. This algorithm makes it possible to determine the value of k on the basis of the Fourier law,

$$k = -\frac{q_z}{dT/dz}, \qquad (2)$$

where q_z and dT/dz are the heat flux and the temperature gradient in the selected direction, respectively. In the Müller–Plathe algorithm, the following procedure is applied to "create" the heat flux.

At the first stage, the studied structure is divided into thin layers. The central layer is called "hot", and one of the external layers is "cold" (see Fig. 2). During the process of dynamic evolution, an atom with the minimum velocity v_h (the kinetic energy) in the "hot" layer and an atom with the maximum velocity v_c in the "cold" layer are regularly determined after a certain number of time steps. Those two atoms are simulated to exchange their velocities (energies), and this procedure is equivalent to the appearance of the heat flux

$$q_z = \frac{1}{2tS} \sum_{N_{\text{transfers}}} \frac{1}{2} M[v_c^2 - v_h^2] \qquad (3)$$

in the structure, where t is the time required for the atoms to exchange their velocities, S the area of the specimen cross-section, and M the mass of each atom. After a good number of velocity exchanges, the average kinetic energy of the atoms in the "hot" layer (and, hence, the temperature of this layer) becomes higher than the average kinetic energy of the atoms (and, hence, the average temperature) over the specimen. Accordingly, the temperature of the "cold" layer becomes lower than the average temperature over the
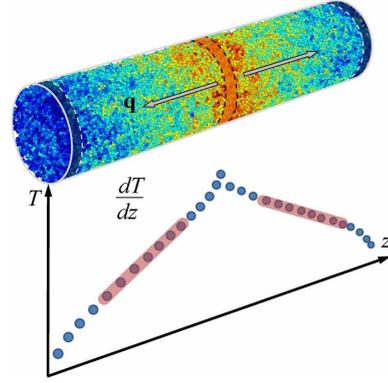

Fig. 2. Scheme explaining the Müller–Plathe algorithm for the determination of the thermal conductivity in a nanowire. In the upper part of the figure, the dashed curves distinguish the central and two outermost layers of the nanowire. The arrows indicate the direction of a heat flow **q** in the structure. The lower part schematically illustrates the temperature distribution along the nanowire. The straight-line sections in the dependence $T(z)$ mark intervals, where the temperature gradient is determined

specimen. The temperature of every i-th layer, T_i, can be calculated from the relation

$$T_i = \frac{1}{t_{\text{av}}} \sum_t \left[\frac{1}{3} N_i k_B \sum_{j=1}^{N_i} M_j v_j^2 \right], \qquad (4)$$

where N_i is the number of atoms in the i-th layer, k_B the Boltzmann constant, and t_{av} the time interval used to calculate the average temperature.

The thermal conductivity was calculated following the Müller–Plathe algorithm, when a stationary heat flux through the structure was established. In this work, the evolution of the total system energy $E(t)$ was analyzed. Its linear dependence testified to the establishment of stationary conditions and a stationary temperature profile $T(z)$ along the specimen. To eliminate the influence of the specimen boundaries, when calculating the temperature gradient dT/dz in the structure, linear sections in the dependence $T(z)$ were selected (see Fig. 2). Now, knowing the values of q_z and dT/dz, the thermal conductivity of the structure can be calculated using formula (2).

3. Results and Their Discussion

At the first stage of studies, we calculated the temperature dependences of the thermal conductivity in Si nanowires with amorphous SiO_2 shells. Figure 3
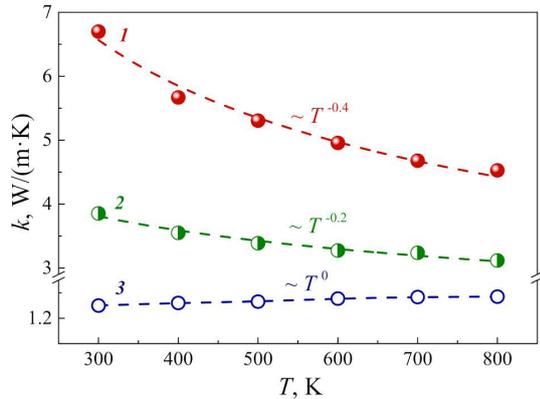
Fig. 3. Temperature dependences of the thermal conductivity coefficient for Si (*1*), Si/SiO$_2$ (*2*), and SiO$_2$ (*3*) nanowires

demonstrates the obtained $k(T)$ dependences for three nanowires with the same radius $R = 3.5$ nm: a crystalline-Si nanowire without any amorphous shell, a Si nanowire with a SiO$_2$ shell 0.5 nm in thickness, and a totally amorphous SiO$_2$ nanowire without any crystalline-silicon core. In the whole examined temperature interval from 300 to 800 K, the silicon nanowire had the highest thermal conductivity, the amorphous SiO$_2$ nanowire was characterized by a minimum k, and the core/shell nanowire revealed intermediate values of its thermal conductivity. As the temperature increased, the thermal conductivity of the Si and Si/SiO$_2$ nanowires monotonically decreased, whereas the value of k for the amorphous SiO$_2$ nanowire practically did not change and remained equal to about $k = 1.3$ W/(m·K), which is close to the thermal conductivity in massive SiO$_2$ [28]. An approximation of the obtained dependences $k(T)$ showed that $k \sim T^{-0.4}$ for the silicon nanowire, $k \sim T^{-0.2}$ for the Si nanowire with the SiO$_2$ shell, and $k \sim T^0$ for the amorphous SiO$_2$ nanowire.

It is known that the phonon thermal conductivity in solids can be estimated by the formula

$$k = \frac{1}{3} c_{\mathrm{ph}} v_{\mathrm{ph}} \lambda_{\mathrm{ph}}, \qquad (5)$$

where c_{ph}, v_{ph}, and λ_{ph} are the heat capacity, velocity, and free path of phonons, respectively. At sufficiently high temperatures, the heat capacity of solids is constant in agreement with the Dulong–Petit law, and the velocity of phonon propagation also weakly varies with the temperature. Therefore, the dependence $k(T)$ at high temperatures is gov-

erned by the temperature dependence of the phonon free path length. As the temperature increases, the phonon-phonon scattering processes become a dominant mechanism that restricts the motion of phonons, and their free path length λ_{ph} is reciprocal to the phonon concentration n_{ph}. On the other hand, since $n_{\mathrm{ph}} \sim T$ at high temperatures, the proportionality $k \sim T^{-1}$ should be obeyed for Si single crystals. This conclusion is confirmed experimentally [30].

When changing from an infinite single crystal to a nanowire, the characteristic size of the system decreases, and another mechanism restricting the motion of phonons becomes active. This is the scattering at the material boundaries. If the characteristic size of the system L becomes comparable to the free path length of phonons, we obtain $\lambda_{\mathrm{ph}} \sim L = $ const and, as a result, $k \sim T^0$. This scenario takes place, e.g., in the amorphous nanowire, where thermal vibrations are confined to a few interatomic distances because of the structural disorder. From the above considerations, it follows that the dependence $k \sim T^{-0.4}$ obtained for the Si nanowire is a result of two competing scattering mechanisms: phonon-phonon screening (with the dependence $k \sim T^{-1}$) and scattering at the lateral surface of nanowire (for which $k \sim T^0$).

A slower variation of the thermal conductivity in the Si/SiO$_2$ nanowire with an amorphous shell, as the temperature grows, can be explained by the following factors. First, the Si/SiO$_2$ nanowire has a smaller radius of its crystalline core in comparison with the silicon nanowire and, accordingly, a smaller volume of the thermally conductive material and a larger specific surface area, which results in a stronger phonon scattering and a simultaneous reduction of the thermal conductivity of the structure. Second, as was shown in work [31], the phonon spectrum of Si/SiO$_2$ heterostructures contains (at $f < 4$ THz) a new low-frequency band of localized vibrations of atoms situated at the Si/SiO$_2$ interface. A random distribution of those vibrational states at the heterointerface of the studied nanowire provokes the additional scattering of thermal vibrations with a corresponding reduction of the k value.

To analyze the influence of the thickness of the SiO$_2$ oxide shell on the thermal conductivity of the nanowire, we calculated the dependences $k(d/R_{\mathrm{core}})$ for SiO$_2$ nanowires with a fixed radius of the crystalline silicon core ($R_{\mathrm{core}} = $ const). The curves $k(d/R_{\mathrm{core}})$ obtained for two nanowires with $R_{\mathrm{core}} = 1.5$ and

3 nm at $T = 300$ K are shown in Fig. 4. The nanowire with a larger radius of its crystalline core has the higher thermal conductivity k in the whole interval of d/R_{core} values. This result can be understood bearing in mind that the nanowire with the smaller R_{core} has a larger specific surface area of the thermally conductive crystalline core, which gives rise to a higher intensity of the phonon scattering at the Si/SiO₂ heterointerface. As the thickness d of the amorphous SiO₂ shell increases, a monotonic decrease in the thermal conductivity k of the analyzed nanowires is observed. The growth of the ratio d/R_{core} from 0.1 to 0.7 brings about an almost 1.5-reduction of the k value for both nanowires.

When explaining such a behavior of the thermal conductivity coefficient, it should be taken into account that heat is transferred in Si/SiO₂ nanowires through two independent channels: the crystalline core and the amorphous shell. The resulting thermal conductivity of the nanowire is determined by the volume fraction of each channel and the value of its own thermal conductivity, and it can be described by the following simple relation [32]:

$$k = \frac{k_{core}R_{core}^2}{(R_{core} + d)^2} + \frac{k_{shell}((R_{core} + d)^2 - R_{core}^2)}{(R_{core} + d)^2}, \quad (6)$$

where the first and second terms on the right-hand side are the thermal conductivities of the core and shell, respectively, times their volume fractions in the nanowire. As follows from the above expression, the increase of the amorphous shell thickness d, provided a constant value of the crystalline core radius R_{core}, enlarges the volume fraction of the material with the low thermal conductivity, which ultimately leads to a reduction of the total thermal conductivity of the nanowire.

The analysis of expression (6) also demonstrates that the total thermal conductivity of Si/SiO₂ nanowires increases with the radius of the crystalline core, if the thickness d of the amorphous SiO₂ shell remains constant. This conclusion is confirmed by the results of calculations that are shown in Fig. 5 for two nanowires with the fixed thicknesses of their SiO₂ shells: $d = 0.5$ and 1 nm.

The thermal conductivity coefficient of the amorphous SiO₂ nanowire ($R_{core} = 0$) is approximately equal to $k = 1.3$ W/(m·K) and increases rapidly with the fraction of the crystalline core in the nanowire. In
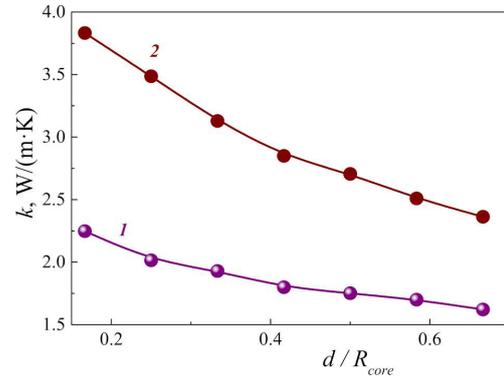

Fig. 4. Dependences of the thermal conductivity in Si/SiO₂ nanowires with the crystalline-core radius $R_{core} = 1.5$ (*1*) and 3 nm (*2*) on the thickness d of the amorphous shell SiO₂, The temperature $T = 300$ K
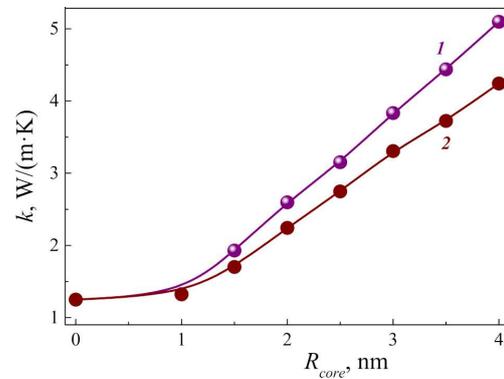

Fig. 5. Dependence of the thermal conductivity in Si/SiO₂ nanowires with a fixed thickness of the amorphous SiO₂ shell $d = 0.5$ (*1*) and 1.0 nm (*2*) on the radius d of the crystalline Si core. The temperature $T = 300$ K

particular, if R_{core} increases to 4 nm, the value of k increases drastically to almost 5 and 4 W/(m·K) in nanowires with $d = 0.5$ and 1.0 nm, respectively. The obtained results testify that the thermal conductivity of Si nanowires can be controlled by varying the thickness of the oxide shell, which can be easily realized when growing those structures.

4. Conclusions

The coefficient of thermal conductivity k in silicon nanowires with an amorphous SiO₂ shell is calculated using the method of nonequilibrium molecular dynamics. By analyzing the obtained temperature dependences $k(T)$, it is shown that the heat transfer processes in the researched Si/SiO₂ nanowires are driven by two competing scattering mechanisms:

phonon-phonon and phonon-boundary screening. It is found that the growth of the thickness of the amorphous SiO_2 shell at a constant radius of the crystalline Si core results in a reduction of the thermal conductivity in the Si/SiO_2 nanowires. On the other hand, if the thickness of the natural oxide layer is fixed, the thermal conductivity of nanowires increases sharply with the radius of the silicon core. The obtained results can serve as a basis for developing the methods aimed at the optimization of thermoelectric transducers based on silicon nanostructures.

1. Y. Cui, Z. Zhong, D. Wang, W.U. Wang, C.M. Lieber. High performance silicon nanowire field effect transistors. *Nano Letters* **3**, 149 (2003).

2. Y. He, W. Yu, G. Ouyang. Shape-dependent conversion efficiency of Si nanowire solar cells with polygonal cross-sections. *J. Appl. Phys.* **119**, 225101 (2016).

3. M.N. Esfahani, Y. Kilinc, M.C. Karakan, E. Orhan, M.S. Hanay, Y. Leblebici, B.E. Alaca. Piezoresistive silicon nanowire resonators as embedded building blocks in thick SOI. *J. Micromech. Microeng.* **28**, 045006 (2018).

4. A.K. Katiyar, A.K. Sinha, S. Manna, S.K. Ray. Fabrication of Si/ZnS radial nanowire heterojunction arrays for white light emitting devices on si substrates. *ACS Appl. Mater. Interf.* **6**, 15007 (2014).

5. Y. Yang, W. Yuan, W. Kang, Y. Ye, Q. Pan, X. Zhang, Y. Ke, C. Wang, Z. Qiu, Y. Tang. A review on silicon nanowire-based anodes for next-generation high-performance lithium-ion batteries from a material-based perspective. *Sustain. Energ. Fuels* **3**, 1 (2020).

6. N.I. Goktas, P. Wilson, A. Ghukasyan, D. Wagner, S. McNamee, R.R. LaPierre Nanowires for energy: A review. *Appl. Phys. Rev.* **5**, 041305 (2018).

7. F. Domínguez-Adame, M. Martín-González, D. Sánchez, A. Cantarero. Nanowires: A route to efficient thermoelectric devices. *Physica E* **113**, 213 (2019).

8. O. Korotchenkov, A. Nadtochiy, V. Kuryliuk, C.-C. Wang, P.-W. Li, A. Cantarero. Thermoelectric energy conversion in layered structures with strained Ge quantum dots grown on Si surfaces. *Eur. Phys. J. B* **87**, 64 (2014).

9. A. Majumdar. Thermoelectricity in semiconductor nanostructures. *Science* **303**, 777 (2004).

10. A.I. Hochbaum, R. Chen, R.D. Delgado, W. Liang, E.C. Garnett, M. Najarian, A. Majumdar, P. Yang. Enhanced thermoelectric performance of rough silicon nanowires. *Nature* **451**, 163 (2008).

11. J. Chen, G. Zhang, B. Li. A universal gauge for thermal conductivity of silicon nanowires with different cross sectional geometries. *J. Chem. Phys.* **135**, 204705 (2011).

12. A. Paul, M. Luisier, G. Klimeck. Shape and orientation effects on the ballistic phonon thermal properties of ultrascaled Si nanowires. *J. Appl. Phys.* **110**, 114309 (2011).

13. J.M. Weisse, A.M. Marconnet, D. Kim, P.M. Rao, M.A. Panzer, K.E. Goodson, X. Zheng. Thermal conductivity in porous silicon nanowire arrays. *Nanosc. Res. Lett.* **7**, 554 (2012).

14. S. Yi, C. Yu. Modeling of thermoelectric properties of SiGe alloy nanowires and estimation of the best design parameters for high figure-of-merits. *J. Appl. Phys.* **117**, 035105 (2015).

15. M. Royo, R. Rurali. Tuning thermal transport in Si nanowires by isotope engineering. *Phys. Chem. Chem. Phys.* **18**, 26262 (2016).

16. M.G. Shahraki, Z. Zeinali Effects of vacancy defects and axial strain on thermal conductivity of silicon nanowires: A reverse nonequilibrium molecular dynamics simulation. *J. Phys. Chem. Solids* **85**, 233 (2015).

17. C.W. Zhang, H. Zhou, Y. Zeng, L. Zheng, Y.L. Zhan, K.D. Bi. A reduction of thermal conductivity of non-periodic Si/Ge superlattice nanowire: Molecular dynamics simulation. *Int. J. Heat Mass Transf.* **132**, 681 (2019).

18. M. Isaiev, O. Didukh, T. Nychyporuk, V. Timoshenko, V. Lysenko. Anisotropic heat conduction in silicon nanowire network revealed by Raman scattering. *Appl. Phys. Lett.* **110**, 011908 (2017).

19. J.P. Feser, J.S. Sadhu, B.P. Azeredo, K.H. Hsu, J. Ma, J. Kim, M. Seong, N.X. Fang, X. Li, P.M. Ferreira, S. Sinha, D.G. Cahill. Thermal conductivity of silicon nanowire arrays with controlled roughness. *J. Appl. Phys.* **112**, 114306 (2012).

20. F. Zhuge, T. Takahashi, M. Kanai, K. Nagashima, N. Fukata, K. Uchida, T. Yanagida. Thermal conductivity of Si nanowires with δ-modulated dopant distribution by self-heated 3ω method and its length dependence. *J. Appl. Phys.* **124**, 065105 (2018).

21. P. Lishchuk, M. Isaiev, L. Osminkina, R. Burbelo, T. Nychyporuk, V. Timoshenko. Photoacoustic characterization of nanowire arrays formed by metal-assisted chemical etching of crystalline silicon substrates with different doping level. *Physica E* **107**, 131 (2019).

22. S. Sarikurt, A. Ozden, A. Kandemir, C. Sevik, A. Kinaci, J.B. Haskins, T. Cagin. Tailoring thermal conductivity of silicon/germanium nanowires utilizing core-shell architecture. *J. Appl. Phys.* **119**, 155101 (2016).

23. M. Hu, K.P. Giapis, J.V. Goicochea, X. Zhang, D. Poulikakos. Significant Reduction of Thermal Conductivity in Si/Ge Core-Shell Nanowires. *Nano Lett.* **11**, 618 (2011).

24. X. Liu, G. Zhang, Q. Pei, Y. Zhang. Modulating the thermal conductivity of silicon nanowires via surface amorphization. *Sci. Chin. Technolog. Sci.* **57**, 699 (2014).

25. S. Plimpton. Fast parallel algorithms for short-range molecular dynamics. *J. Comput. Phys.* **117**, 1 (1995).

26. J. Tersoff. Modeling solid-state chemistry: Interatomic potentials for multicomponent systems. *Phys. Rev. B* **39**, 5566 (1989).

27. V. Kuryliuk, S. Semchuk. Molecular dynamics calculation of thermal conductivity in a-SiO₂ and an a-SiO₂-based nanocomposite. *Ukr. J. Phys.* **61**, 835 (2016).

28. V.V. Kuryliuk, O.A. Korotchenkov. Atomistic simulation of the thermal conductivity in amorphous SiO₂ matrix/Ge nanocrystal composites. *Physica E* **88**, 228 (2017).

29. F. Müller-Plathe. A simple nonequilibrium molecular dynamics method for calculating the thermal conductivity. *J. Chem. Phys.* **106**, 6082 (1997).

30. C.J. Glassbrenner, G.A. Slack. Thermal conductivity of silicon and germanium from 3 K to the melting point. *Phys. Rev.* **134**, A1058 (1964).

31. T. Zushi, K. Ohmori, K. Yamada, T. Watanabe. Effect of a-SiO₂ layer on the thermal transport properties of (100) Si nanowires: A molecular dynamics study. *Phys. Rev. B* **91**, 115308 (2015).

32. M. Hu, X. Zhang, K.P. Giapis, D. Poulikakos. Thermal conductivity reduction in core-shell nanowires. *Phys. Rev. B* **84**, 085442 (2011).

В.В. Курилюк, С.С. Семчук,
А.М. Курилюк, П.П. Когутюк

ТЕПЛОПРОВІДНІСТЬ Si
НАНОНИТОК З АМОРФНОЮ SiO₂ ОБОЛОНКОЮ:
МОЛЕКУЛЯРНО-ДИНАМІЧНИЙ РОЗРАХУНОК

Методом нерівноважної молекулярної динаміки досліджено процеси теплового транспорту в Si нанонитках, покритих оболонкою аморфного SiO₂. Розглянуто вплив товщини аморфного шару, радіуса кристалічного кремнієвого ядра і температури на величину коефіцієнта теплопровідності нанониток. Встановлено, що збільшення товщини аморфної оболонки зумовлює зменшення теплопровідності Si/SiO₂ нанониток типу ядро-оболонка. Результати також показують, що теплопровідність Si/SiO₂ нанониток при 300 К зростає зі збільшенням площі поперечного перерізу кристалічного Si ядра. Виявлено, що температурна залежність коефіцієнта теплопровідності Si/SiO₂ нанониток типу ядро-оболонка є суттєво слабшою, ніж в кристалічних кремнієвих нанонитках. Показано, що така відмінність є результатом різних домінуючих механізмів фононного розсіювання в нанонитках. Отримані результати демонструють, що нанонитки Si/SiO₂ є перспективним матеріалом для термоелектричних застосувань.

К л ю ч о в і с л о в а: коефіцієнт теплопровідності, нанонитка, кремній, молекулярна динаміка.